Copyright Warning & Restrictions

The copyright law of the United States (Title 17, United States Code) governs the making of photocopies or other reproductions of copyrighted material.

Under certain conditions specified in the law, libraries and archives are authorized to furnish a photocopy or other reproduction. One of these specified conditions is that the photocopy or reproduction is not to be "used for any purpose other than private study, scholarship, or research." If a, user makes a request for, or later uses, a photocopy or reproduction for purposes in excess of "fair use" that user may be liable for copyright infringement,

This institution reserves the right to refuse to accept a copying order if, in its judgment, fulfillment of the order would involve violation of copyright law.

Please Note: The author retains the copyright while the New Jersey Institute of Technology reserves the right to distribute this thesis or dissertation

Printing note: If you do not wish to print this page, then select "Pages from: first page # to: last page #" on the print dialog screen

ABSTRACT

Title of Thesis: The Heterogeneous Catalytic Decomposition of Isopropyl Alcohol Over 0.5% Platinum on 4-8 Mesh Charcoal Catalyst Support

Thomas Michael Kudenchak, Master of Science in Chemical Engineering, 1981

Thesis directed by: Dr. Deran Hanesian, Professor of Chemical Engineering

The heterogeneous catalytic decomposition of isopropyl alcohol vapor over 0.5% platinum on (4-8 mesh) charcoal support catalyst was studied at bench-top in a fixed-bed tubular microreactor of about 1 cm ID, six inches long containing one or two grams of catalyst. Reactor feed and exit gas analysis was obtained by gas chromatography.

Experimental runs aimed at determining the Arrhenius parameters and the reaction order (assuming the applicability of a simple power law model) were performed with 1 and 2 grams of catalyst at various residence times ranging from 0.24 to 2.3 seconds and temperatures of 150°, 175°, 200°, 225°, and 250 degrees Celsius. In addition, a short study of the reaction selectivity (as impacted by temperature only) was made for reactor temperatures ranging from 100° to 400°C.

Because all runs were operated under laminar flow conditions, the specific reaction rate constants were calculated from both the plug flow and the dispersion models. A comparison

of corresponding k-values between the two methods revealed no statistically significant difference despite the fact that the dispersion group had indicated moderate dispersion ($0.025 \leq \frac{D_z}{v_s L} \leq 0.05$).

Finally, severe catalyst decay observed at both high ($400^{o}C$) and low ($150^{o}C$) temperature levels narrowed the range of study to the above temperature conditions. Although the actual causes of catalyst deactivation remain inconclusive, sintering and fouling are felt to be responsible for high and low temperature decays, respectively.

THE HETEROGENEOUS CATALYTIC DECOMPOSITION OF ISOPROPYL ALCOHOL OVER 0.5% PLATINUM ON 4-8 MESH CHARCOAL CATALYST SUPPORT

by

Thomas Michael Kudenchak

Thesis submitted to the Faculty of the Graduate School of the New Jersey Institute of Technology in partial fulfillment of the requirements for the degree of Master of Science in Chemical Engineering
1981

APPROVAL SHEET

Title of Thesis: The Heterogeneous Catalytic Decomposition of Isopropyl Alcohol Over 0.5% Platinum on 4-8 Mesh Charcoal Catalyst Support

Name of Candidate: Thomas Michael Kudenchak
Master of Science in Chemical Engineering, 1981

Thesis and Abstract Approved:

_____ , _____
Dr. Deran Hanesian Date
Professor & Chairman
Department of Chemical
Engineering & Chemistry

Date

VITA

Name: Thomas Michael Kudenchak

Permanent address:

Degree and date to be conferred: Master of Science in Chemical Engineering, 1981

Date of birth:

Place of birth:

Secondary education: Hudson Catholic High School, Jersey City

Collegiate institution attended	Dates	Degree	Date of Degree
New Jersey Institute of Technology	1974-78	BS ChE	1978
New Jersey Institute of Technology	1978-81	MS ChE	1981

Major: Chemical Engineering

Positions held:

1978-79	Teaching Assistant, New Jersey Institute of Technology, Newark, New Jersey
1979-Present	Assistant Chemical Engineer, Technical Research, Maxwell House, General Foods, Hoboken, New Jersey

ACKNOWLEDGMENTS

The author would like to express sincere appreciation to the following for their most generous assistance in making this study possible.

Mr. Joseph Kisutcza

Mr. Edward Karen

Dr. James Grow

Dr. Subash Dutta

Dr. William Snyder

My special thanks go to Dr. Deran Hanesian, my advisor, for sacrificing much of his time and effort in helping me over many hurdles experienced throughout this study.

TABLE OF CONTENTS

LIST OF TABLES

LIST OF FIGURES

CHAPTER I

INTRODUCTION

GENERAL INTRODUCTION

An aspiring aim of catalytic research is to develop a unified theoretical model that can reliably formulate the performance of most solid-support catalysts. Although knowledge in this field has grown dramatically in recent times, the act of selecting these catalysts for specific industrial processes remains, for the most part, more an art than a science. This fact is profoundly evident by the empirically based trial and error approach frequently employed whenever searching for new catalysts, or performance testing of existing ones.

Many obstacles blocking formulation rest not so much on insufficient thecretical know-how (though there are such aspects as the kinetics of surface reaction mechanisms not yet fully understood) but rather with the broadly varied physical properties that uniquely characterize each catalyst and support. These properties range from pore size, pellet size, shape, and surface area, down to catalyst concentration and dispersion within the support, and finally, to the minutest detail of surface charge and crystalline structure. However, these factors alone do not wholely predetermine a catalyst's effectiveness. Instead, it is the complex interaction of the above (together with factors not yet mentioned) within the reaction environment that will ultimately decide the end pro-

duct. Thus, for reason of sheer complexity alone, it is eminently impractical to formulate the performance of any given catalyst via pure theory.

Nonetheless, in assessing a catalyst's performance the existing theory of solid-fluid catalysis does become a potent tool when paired with top quality bench-top experimentation. Though much like a tool, the theory too has great utility, but in enabling the versatile treatment of experimental kinetic data to effect formulation.

At the one extreme (from the standpoint of the catalytic researcher in search of a firm understanding of the observed reaction phenomena) raw data is treated in a rigorous fashion typified by first posing a suitable mechanistic expression, and then applying one of many available facilitative computer-aided correlation techniques. It should be noted, however, that such an approach at the outset has no real guarantee of success. For as can conceivably occur, substantial experimental error may mask the effect being studied, and thereby lead to faulty findings. In order to insure experimental integrity, it is necessary to obtain a statistically sufficient quantity of data. In most cases, however, getting a sufficient amount of data comes at the expenditure of much time and effort.

At the other extreme (from the standpoint of the design engineer constrained by time and economics, and chiefly concerned with preliminary reactor design), the theory lends itself to a more simplistic, yet nevertheless valid way of developing a kinetic rate expression. It involves regressing

experimental data to first and/or second order homogeneous equations, and then selecting that expression which fits well. Although the resulting equation reveals little about the true nature of the reaction mechanism, it does allow the engineer to interpolate reaction rates though within the limits of experimental operating conditions.

In summary, due to the complicated nature of solid-fluid reactions, the existing catalytic theory alone is inadequate to predict a catalyst's performance. Therefore it must be supplemented with experimentation. The treatment of raw data to achieve formulation can be as complex, but also provides considerable flexibility to meet the needs of the investigator.

DECOMPOSITION OF ISOPROPYL ALCOHOL

The gas phase decomposition reaction of isopropyl alcohol over 0.5% platinum on charcoal was investigated in a fixed-bed tubular micro-reactor. Initial test plans were (1) to establish the reaction order, (2) to determine the activation energy and pre-exponential factor, and (3) to observe the reaction selectivity--all at various flow rates and reactor temperatures (T) ranging from 100 to 400°C. However, severe catalyst deactivation experienced early on in the study at both high and low temperature levels precluded work over the full temperature range. Nevertheless, the above objectives were still met although lessened somewhat in scope.

As a means of evaluating rate parameters and reaction order, the plug flow and dispersion models were employed to determine the specific reaction rate constants (k) and reaction order since flow conditions in the packed bed were laminar ($N_{Re} \leq 40$). Regression analysis of data gave the activation energy and pre-exponential factor.

A survey of recent literature in Chemical Abstracts was made and the results revealed little published information on the catalyst used in this study. Consequently, many of the conclusions (on topics such as catalyst deactivation) were drawn from other studies with different catalyst but similar problems.

CHAPTER II

THEORY

SOLID-FLUID CATALYSIS

CONTINUOUS REACTION MODEL

Before a solid-catalyzed gas-phase reaction can occur, the reactant (IPA) must first reach an active (Pt) catalyst site. These sites lie on the gas-solid interfaces of the exterior surface, and also the interior surface within pores. Although the pores are singly small in size, their vast number offers an active surface area many times that of the outer surface. In order to reach these inner sites, however, the reactant must first overcome resistances opposing its inward diffusion.

To better understand this phenomena, a continuous reaction model is used. It assumes an overall reaction occurs in seven distinct steps. In this case, the slowest step of this ideal model is reaction rate controlling. These steps are listed and briefly described below in progressive order.

1. Gas Film Diffusion of Reactants

Reactant (IPA) diffuses from bulk gas stream into a gaseous boundary film layer which envelops the support's outer surface.

2. Pore Diffusion of Reactants

Reactant approaches pore mouth on outer support surface, migrates inward driven by concentration gradient.

3. Adsorption of Reactants

Reactant impacts inner surface and is adsorbed onto an active site.

4. Surface Reaction

Reactant catalytically decomposes and is converted to products.

5. Desorption of Products

Products desorb from site. (This event reactivates site for next decomposition.)

6. Pore Diffusion of Products

Products then diffuse outward towards pore mouth.

7. Gas Film diffusion of Products

Products diffuse from gaseous boundary film layer and are swept away into the bulk gas stream.

Any of these seven steps can be rate determining and will result in various forms of the rate law.

CATALYST DEACTIVATION

Ideally, the principal role of a catalyst is to speed up the rate of a reaction without itself becoming consumed or altered by the reaction process. However, if this were true in practice, there would be no net loss in potency with on-stream usage. Unfortunately, most catalysts do in fact demonstrate diminished activity. The extent of this degradation along with its swiftness and severity depends largely upon the type of deactivation involved as well as the reaction environment.

For example, some catalysts are known to undergo structural changes as a consequence of exposure to high temperature. When the catalyst sites cluster and/or the support surface agglomerates due to prevailing harsh thermal conditions, the term 'sintering' is applied. The devastating effects of a sintering catalyst can be as pronounced as a sharp plunge in yield and/or an altered reaction selectivity. In most instances, however, a sintered catalyst suffers permanent damage.

Other types of deactivation include carbon deposition, fouling, and catalytic chemisorption poisoning. However, these will be described later with regards to their possible connection with this study. (See experimental results-catalyst deactivation.)

REACTION SELECTIVITY

The decomposition reaction of isopropyl alcohol (IPA) vapor over 0.5% platinum on charcoal (4-8 mesh) demonstrates a marked change in selectivity with reaction temperature. For example, at low temperature levels and short residence times IPA dehydrogenates to give acetone and hydrogen as its principal products. Whereas for conditions of high temperature and long residence time, the predominant reaction is one of dehydration by which propylene and water are yielded. These two reactions appear as follows:

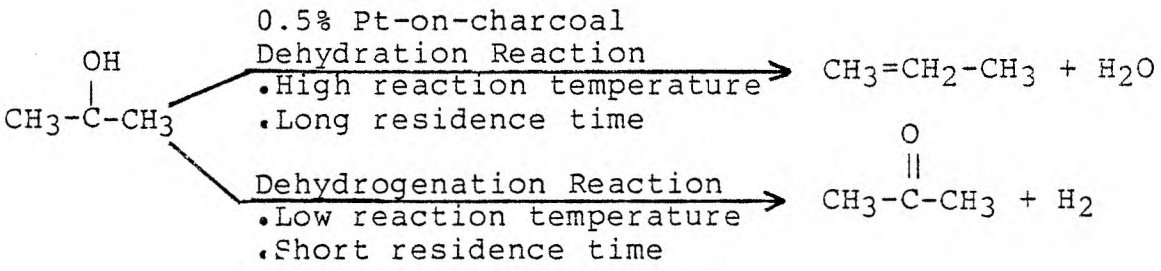

Although there are two competing reactions occurring simultaneously, only the dehydrogenation reaction is important for the temperature region studied (150°C - 250°C).

PLUG FLOW MODEL (PFM)[7]

Where little or no axial mixing occurs throughout the fixed-bed tubular reactor, the PFM can be suitably applied to determine the specific reaction rate constant (k) and reaction order. The general equation, with k expressed in terms of bed void volume, takes on the following familiar form:

$$\varepsilon \frac{V_b}{F_{ai}} = \int_{X_i=0}^{X_{af}} \frac{d\ X_a}{(-r_a)} \qquad (1)$$

By assuming first order kinetics, and a constant volume system,

$$\varepsilon \frac{V_b}{F_{ai}} = \int_{0}^{X_{af}} \frac{d\ X_a}{k\ C_a} \qquad (2)$$

Since $F_{ai} = (v_i)(C_{ai})$ and $C_a = C_{ai}(1 - X_a)$, the equation reduces to the following form after integration:

$$\tau = \varepsilon \frac{V_b}{v_i} = - \frac{Ln(1 - X_a)}{k}$$

or

$$k = \frac{Ln(1 - X_a)}{\tau} \qquad (3)$$

DISPERSION MODEL[7]

When the dispersion number (D_z/v_sL) exceeds 0.025, the impact of axial mixing on conversion cannot be ignored. The general equation accounting for axial dispersion (in terms of fractional conversion) has the following form

$$\frac{D_z}{v_sL}\frac{d^2X_a}{dZ^2} - \frac{dX_a}{dZ} + k\tau Ca_i^{n-1}(1 - X_a)^n = 0 \qquad (4)$$

Applying the boundary conditions and assuming first order kinetics (n = 1), the solution to this second order linear differential equation is:

$$\frac{C_a}{Ca_i} = 1 - X_a = \frac{4a\ \exp\ (\frac{1}{2}\frac{v_sL}{D_z})}{(1 + a)^2\exp(\frac{a}{2}\frac{v_sL}{D_z}) - (1 - a)^2\exp(-\frac{a}{2}\frac{v_sL}{D_z})} \qquad (5)$$

with

$$a = \sqrt{1 + 4k\tau(D_z/v_sL)} \qquad (6)$$

These equations can be used to determine the specific rate constant, k, based upon the dispersion model.

CHAPTER III

EXPERIMENTAL APPARATUS

SYSTEM DIAGRAM

Figure 1 is a schematic system diagram showing the key flow lines as well as the apparatus used in this study. As a supplement to this diagram, pictures taken of the actual bench-top arrangement are presented in figure 2.

REACTOR FEED SYSTEM

The reactor feed stream consisted of an inert helium carrier gas saturated with isopropyl alcohol (IPA) vapor. Saturation was achieved by bubbling helium (supplied at 50 psig off a pressure regulator valve atop cylinder "A") through liquid IPA held in two cylindrical spargers (E) operated in series. A porous stone plug was inserted at the ends of each sparger feed line to induce suitable fluid-bubble contact. Steady flow control was obtained using a needle valve flowmeter (C). Precise flow measurements were made with the bubble buret (K).

REGENERATION SYSTEM

Before each set of runs, pure helium was allowed to flow through the sparger by-pass needle valve (D) overnight at about 25 cc/min. The purge stream was directed to the fixed-bed reactor via the Valco six-way valve (G).

FIGURE 1. **HETEROGENEOUS CATALYSIS**

SYSTEM DIAGRAM

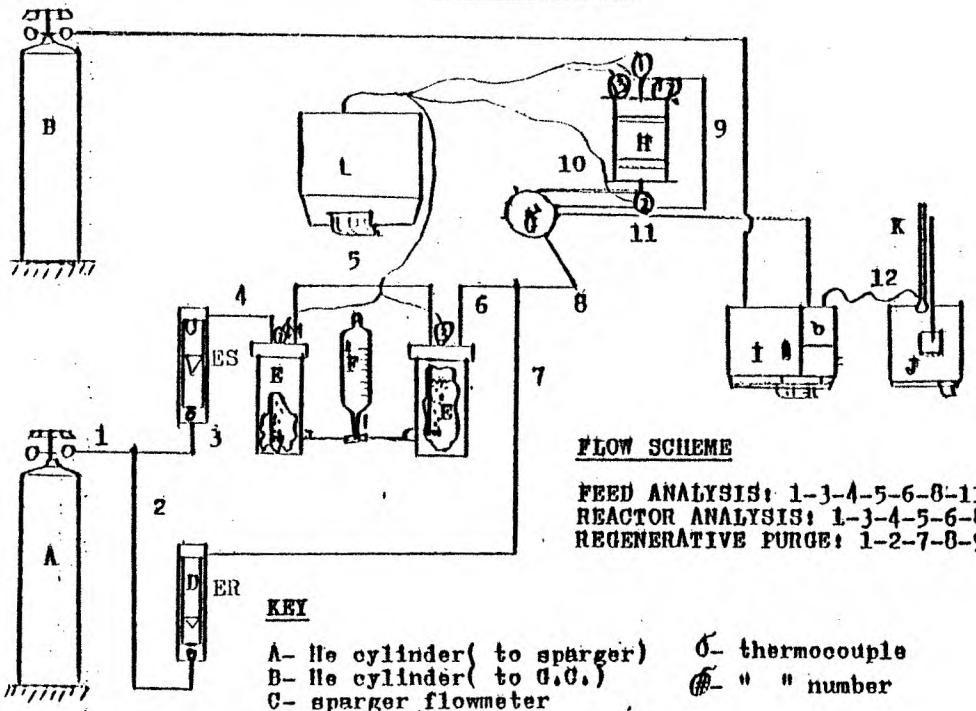

FLOW SCHEME

FEED ANALYSIS: 1-3-4-5-6-8-11-12
REACTOR ANALYSIS: 1-3-4-5-6-8-9-10-11-12
REGENERATIVE PURGE: 1-2-7-8-9-10-11-12

KEY

A- He cylinder(to sparger)
B- He cylinder(to G.C.)
C- sparger flowmeter
D- bypass flowmeter
E- sparger
F- isopropyl reservoir
G- six way valve
H- reactor
I- gas chromatograph & recorder
L- temperature recorder
J- integrator
K- soap bubble buret

σ- thermocouple
(#)- " " number

T. KUDENCHAK '71

FIGURE 2. PHOTOGRAPHS OF EXPERIMENTAL BENCH-TOP SET-UP

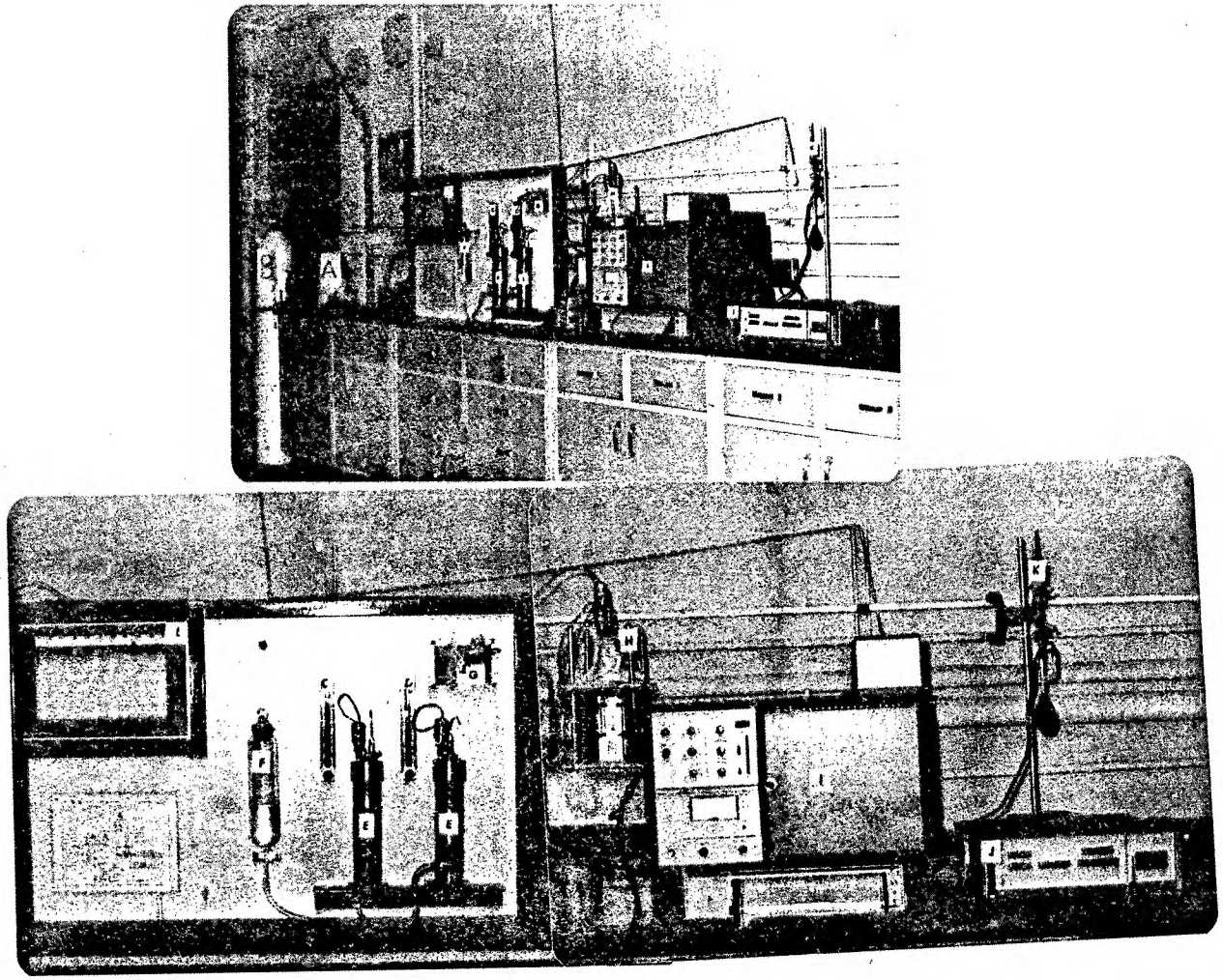

THE REACTOR

Figure 3 illustrates the physical dimensions of the fixed-bed catalytic micro-reactor employed in this study. It was designed from a 2" O.D. x 6" length type 316 stainless steel (s.s.) solid cylindrical rod. A 25/64" diameter hole was drilled dead center which chambered the catalyst bed. The bed was upheld by a fine mesh screen (s.s.) spot-weld to a removable 3/8" O.D. (s.s.) tube. Another screen was placed on top of the bed demarcating the upper chamber boundary. There were two bare wire tip iron-constantan thermocouples inserted at each end of the reactor; one in the effluent gas stream just beneath the bed, and another in the feed stream just above the bed. These temperature probes were connected to a chart recorder for instant temperature read out.

Not shown in figure 2 (to improve overall clarity) are the feed gas preheat tube and the heating coil. The former consisted of a ten foot (straight length) 1/4" s.s. tubing wound around--but not contacting--the reactor exterior. Sandwiched between the preheat tube and wrapped around the reactor exterior was 20 feet of ceramic beaded nichrome wire. A variac was used to regulate electrical power to the heating coil which, in effect, controlled the reactor temperature. Other equipment details are shown in Table 1.

FIGURE 3. KEY REACTOR FEATURES

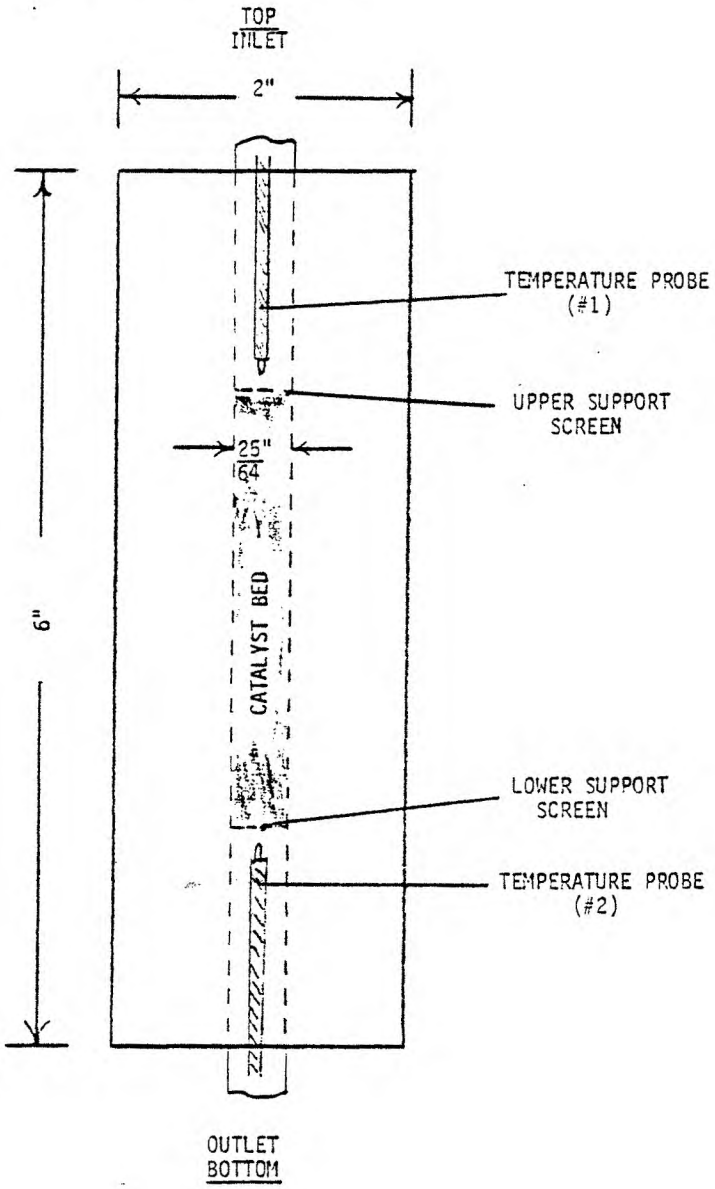

TABLE 1

Material and Equipment Specifications

Temperature Recorder	
Manufacturer	Honeywell Co.
Type	Electronic 112
Range	0-500 C
Model No.	Y11240180-53020-00000-00-00000-(702)-19 OPT 002-101
Serial No.	U3486893001
Flowmeters	
Manufacturer	Brooks Instrument Division Emerson Electric Co.
Model No.	1355CB1C1AAA
Serial No.	7906H78422/1&2
Six-Way Valve	
Manufacturer	Valco Instruments Co. Houston, Texas
Type	Six-Way Valve (1/8" Connections)
Gas Chromatograph	
Manufacturer	Hewlett-Packard
Type	Gas Chromatograph (TC)
Model No.	5700A
Accessories	Chart Recorder 7123A Oven Temp Programmer 5702A Controller Carrier Flow A & B 18714A Two 1/2 cc Sampling Loops
Chromatographic Columns	
Manufacturer	Supelco Inc.
Description	10% Carbowax 20M
Mesh	60/80
Column Size & Material	1/8" dia x 7.5' length stainless steel
Integrator	
Manufacturer	Hewlett-Packard
Type	Integrator
Model No.	3373B

TABLE 1 (Cont'd.)

Material and Equipment Specifications

Reactor

Material of Construction	Type 316 stainless steel
Length	6 in.
O.D.	2 in.
I.D. (Bed Chamber)	25/64 in.

Powerstat

Manufacturer	Superior Electric Co.
Input	120 volts, 50/60 cps
Output	0-135 volts
Amps, Max.	7.5

Heater

Manufacturer	Marsh Beaded Heaters Angleton, TX 77515
Length	20 ft.
Watts	600
Volts	115
Heater Temp., Max.	1093°C

Syringe

Manufacturer	Hamilton Co., Reno, Nevada
Type	Microliter
Model No.	7101

Catalyst Supplier Specifications

Vendor	Englehard Minerals & Chemicals Chemicals & Catalyst Division 429 Delancy Street Newark, New Jersey 07105
Type	0.5% Platinum on Charcoal 4-8 Mesh Carbon
Amount	150 grams
Lot No.	23,718

Isopropyl Alcohol Supplier Specifications

Vendor	Fisher Scientific Co. Chemical Mfg. Div. Fairlawn, New Jersey 07410
Formula Weight	60.10

TABLE 1 (Cont'd.)

Material and Equipment Specifications

Isopropyl Alcohol Supplier Specifications (Cont'd.)

Color (APHA)	5
Neutrality	P.T.
Boiling Point	82.2°C 1
Boiling Range	82.2-82.5°C
Density (g/ml) @ 25°C	0.781
Heavy Metals (as Pb)	0.2 PPM
Nickel (Ni)	0.01 PPM
Residue After Evaporation	0.0002%
Copper (Cu)	0.01 PPM
Iron (Fe)	0.02 PPM
Water (H_2O)	0.1%
Lot No.	783266
Certified	ACS Grade (1 gal)

CHAPTER IV

EXPERIMENTAL PROCEDURE

GENERAL OPERATING PROCEDURE

Helium carrier gas is bubbled through two series connected spargers filled with liquid isopropyl alcohol at room temperature. The sparger off-gas (or now the reactor feed stream) consists of helium saturated with IPA vapor. A six-way valve routes this stream either to the reactor (for subsequent reaction) or to the gas chromatograph (for feed gas analysis). In the former case, the feed stream enters the top of the reactor, flows downward through the catalyst bed, out the bottom of the reactor, through a 1/2 cc sampling loop, and finally out the vent. Similarly, in the later case, the reactor feed stream bypasses the reactor, flows through the sampling loop before being vented. Periodically helium carrier gas is swept through the loop flushing its contents to the Carbowax column for chromatographic analysis. Flow rates of IPA ranged from 5×10^{-5} to 4×10^{-4} gm moles/minute. Total flow rates were 70 to 330 cc/minute at reactor conditions giving residence times of 0.25 and 2.3 seconds. Reactor temperatures were controlled between 150°C and 250°C and the reactor pressure was atmospheric. Reactor runs were made with both 1 gram and 2 gram quantities of 0.5% platinum on 4-8 mesh charcoal catalyst base. A more detailed operating procedure is given in Appendix A.

CHAPTER V

EXPERIMENTAL RESULTS AND DISCUSSION

CATALYTIC DEACTIVATION

A series of runs were performed prior to the proposed experiment (determining the Arrhenius parameters) to evaluate and improve the operating procedure, as well as ascertaining overall system performance. With the exception of reactor temperature, all conditions such as flowrate, catalyst weight and room temperature were identical. During the first two runs, the reactor temperature was slowly raised at a rate of 1.5°C/-min. When the target temperature was reached, a portion of the reactor off-gas was sent to the chromatographic column for analysis. The results of those runs yielded irreproducible data hypothesized to stem from unsteady-state reactor temperature control. A new method was then employed whereby reactor temperature was kept constant so that the system reached steady-state at each sampling temperature. Fresh catalyst (of identical weight) replaced the previously spent catalyst and three runs were made under this new procedure. Findings from those runs, however, supported those of the first two runs in that the data was again irreproducible. The likelihood of catalyst decay emerged upon correlating data and observing the trend of shifting curves (see figure 4).

As shown by figure 4, which is a plot of temperature versus weight percents acetone, propylene, and IPA for two of the runs,

Figure 4. REACTION SELECTIVITY AS IMPACTED BY CATALYST DECAY

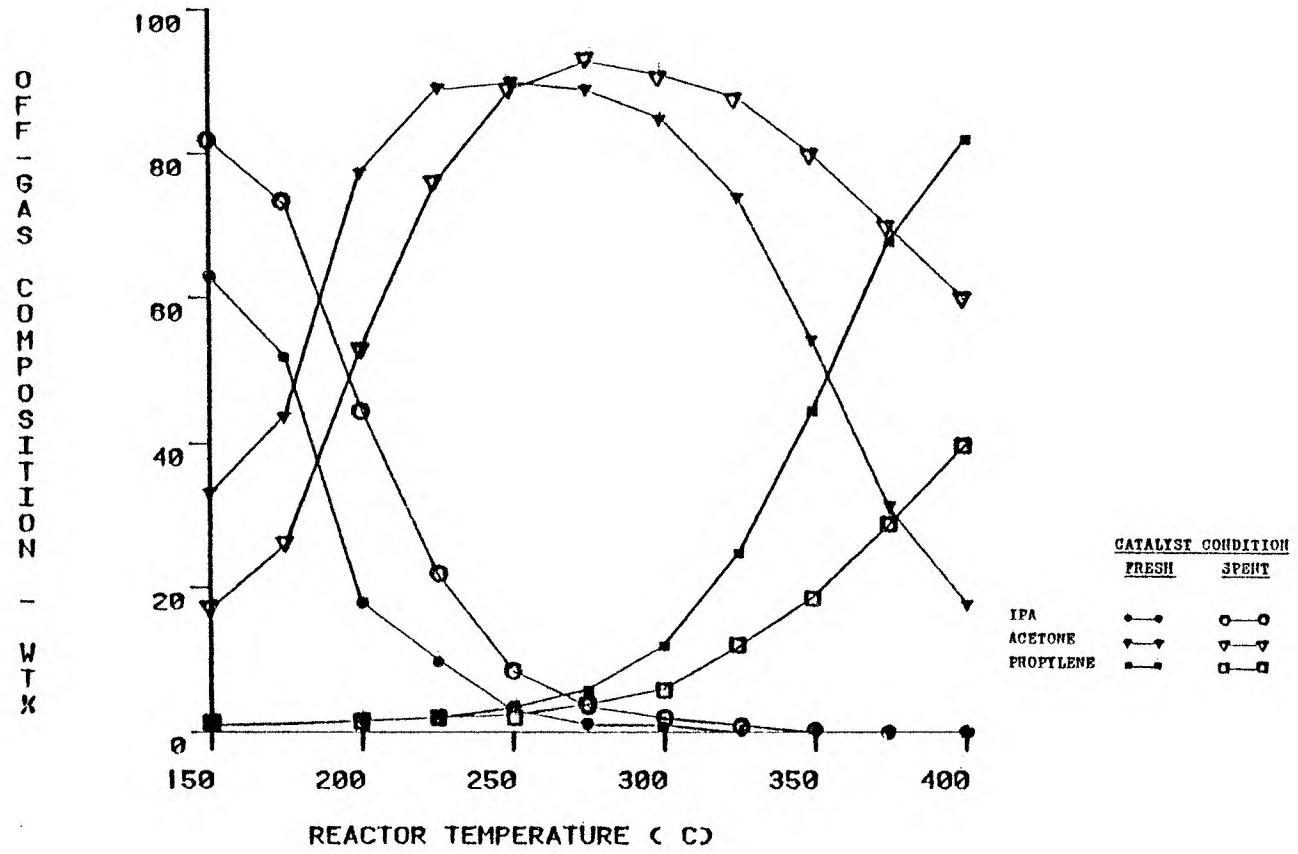

decay was evident by shifting curves with catalyst deactivation indicated by the increased temperatures required for identical conversions. In other words, in order to attain the same activity under similar conditions, a higher temperature was necessary with each successive run. (It should be noted also that weight fraction of acetone was alone a quick and reliable indicator of catalyst activity up to 250°C where acetone was the principal product.)

At this time, the fact that the catalyst was deactivating prevented efforts to determine the Arrhenius parameters. Postulation and then experimental testing for various types of catalyst decay were the next steps taken to understand and reduce the catalyst's diminishing potency. Upon reviewing the literature, the following four types of catalyst deactivation were regarded likely:

1) Fouling
2) Carbon Deposition
3) Sintering
4) Catalytic Chemisorption Poisoning

Fouling

The chief cause of deactivation at lower temperatures (100-150°C) was hypothesized to be the adsorption and retention of either reactant or product on the carbon support surface. Although not proven, fouling was believed to plug the pores of the carbon; thus retarding the transfer of reactant (or product) to (or from) the active platinum sites. There were two

steps taken to successfully solve this problem. These were: (1) the installation of a regenerative purge and (2) the increase in the minimum operating temperature.

The regenerative purge was installed in an effort to clean thermally the catalyst before each run. This installation included the insertion of a sparger bypass line so that pure helium could be fed directly to the reactor. The catalyst was successfully regenerated by this process which required nearly ten hours at temperatures slightly above 300°C. This observed deactivation at low temperatures prompted work to continue at higher temperatures (300-400°C). The results of those runs had indicated yet another type of deactivation, but of a permanent nature.

Carbon Deposition

Carbon deposition was not believed to be a contributing cause of deactivation at low temperatures for the following reasons:

1) Carbon deposition is unlikely to occur at low temperatures.
2) Catalyst deactivation decreased and eventually ceased at higher temperatures (225°C). This was contrary to what can be expected if carbon deposition had prevailed.
3) The catalyst was regenerated in an inert atmosphere and one not condusive to combustion. A combustible environment would have been a requisite for catalyst regeneration had carbon deposition occurred.

Although carbon deposition was not suspect at low temperatures, it might have occurred at higher temperatures (400°C). Unfortunately, deactivation due to carbon deposition could not be tested because of the combustible nature of the catalyst support.

Sintering

At high temperature conditions, it is possible that sintering--the agglomeration of catalyst sites resulting in a reduced surface area--may have occurred. This phenomenon was observed and reported by Dr. Thomas R. Hughes who had worked with the platinum/alumina supported catalyst[5]. In his study, Dr. Hughes concluded that sintering was the major cause of catalyst decay for the alumina support. Since charcoal is a softer support than alumina, it was felt by this author to be even more sinterable. (See figure 5 for typical high temperature catalyst deactivation curve.)

An unsuccessful attempt was made to view the effects of sintering by comparing both fresh and spent catalyst samples under the electron microscope. Although the catalyst pores are easily visible, the effects of sintering remained undetectable at the magnification employed. Trying to boost the magnification beyond 6000X resulted in distortion and blurred images (see figure 6).

Catalytic Chemisorption Poisoning

Some unknown contaminant or poison either in the feed or on the catalyst was considered possible. However, both fresh

Figure 5. TYPICAL HIGH TEMPERATURE (400 C) DEACTIVATION CURVE

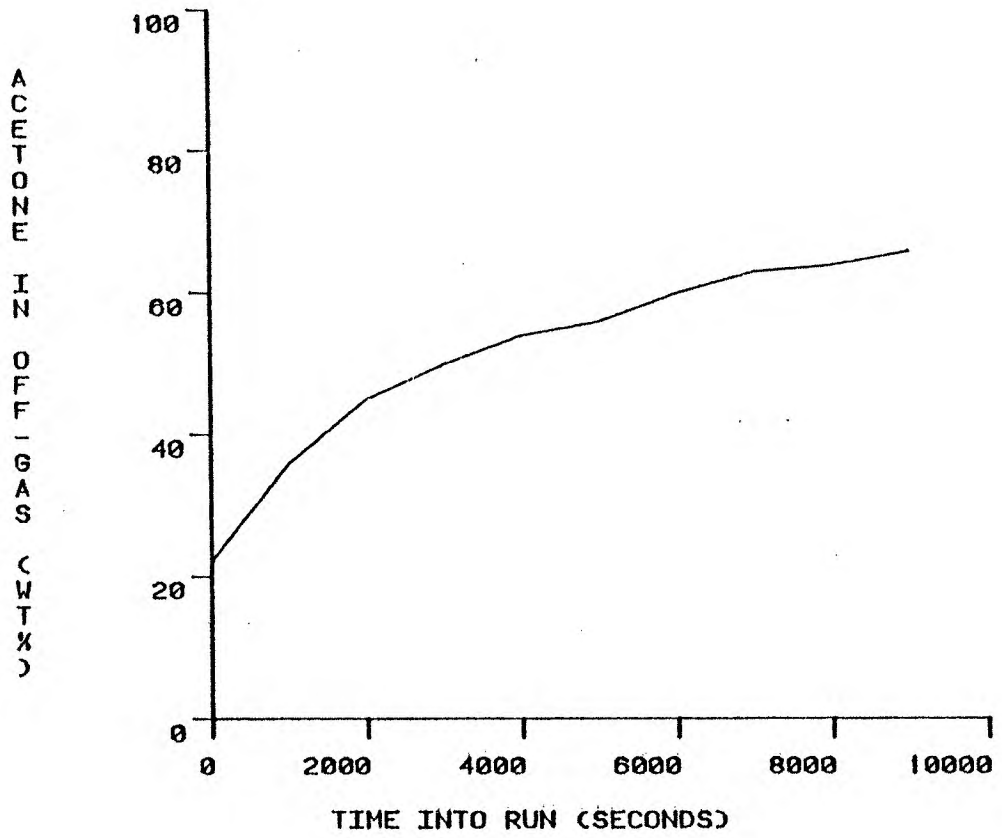

FIGURE 6. PHOTOGRAPHS OF FRESH AND SPENT CATALYST
EMPLOYING ELECTRON MICROSCOPY

FRESH CATALYST
6000 X

SPENT CATALYST
6000 X

and spent catalyst samples were run on ESCA (Electron Scanning Chemical Analysis) revealing no traces of potentially harmful elements (see figure 7).

FIGURE 7. ESCA COMPOSITE SPECTRA OF FRESH AND SPENT CATALYST

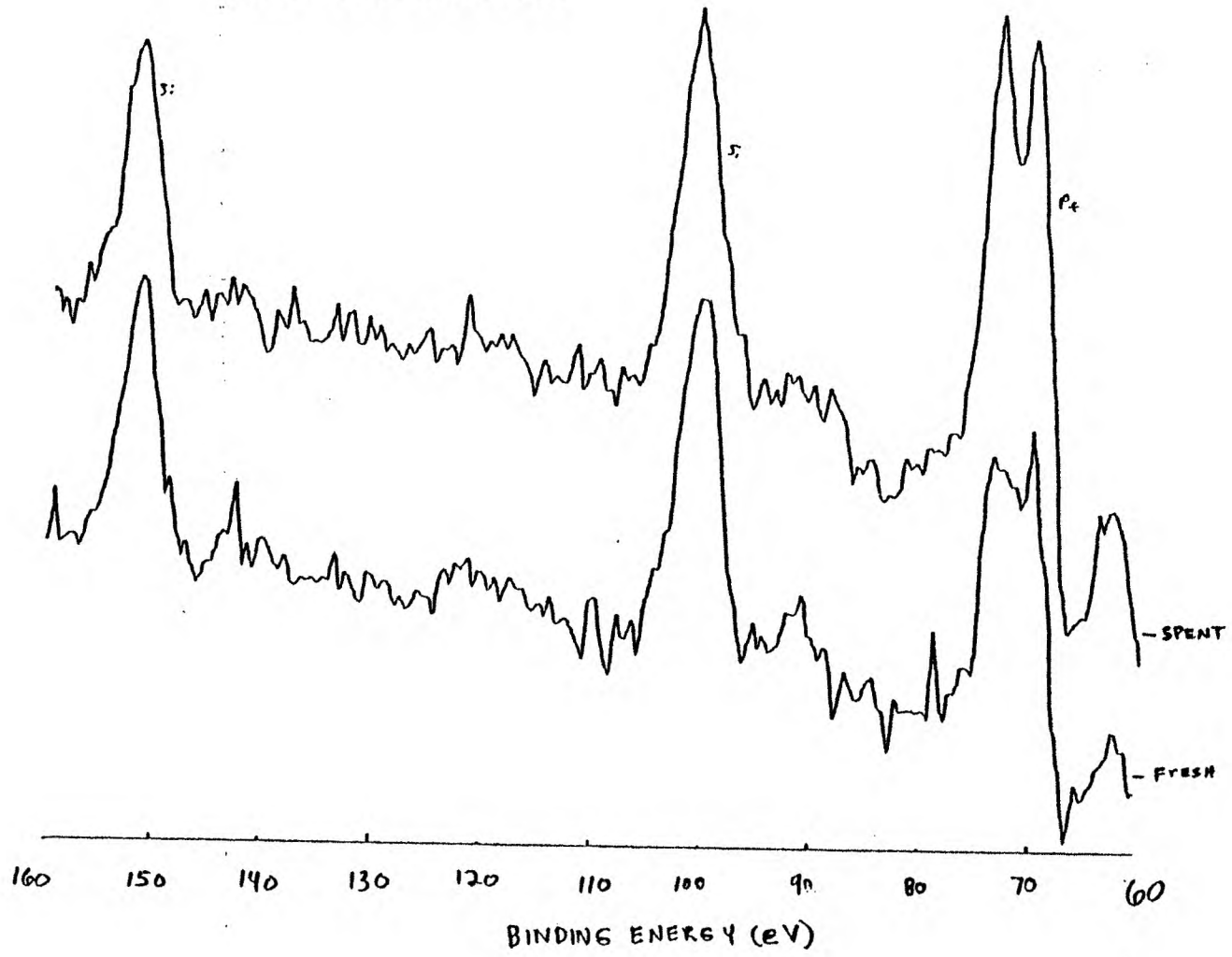

SELECTIVITY

The decomposition reaction of isopropyl alcohol (IPA) over the 0.5% platinum on charcoal catalyst exhibited a large change in selectivity at temperatures above 250°C. Formation to acetone (by dehydrogenation) was prevalent at low temperatures (below 250°C) and short contact times, whereas propylene (by dehydration) was favored at high temperatures (above 350°C) and longer contact times. Figure 8 depicts the reaction selectivity as a function of temperature.

Figure 8. REACTION SELECTIVITY AS A FUNCTION OF TEMPERATURE

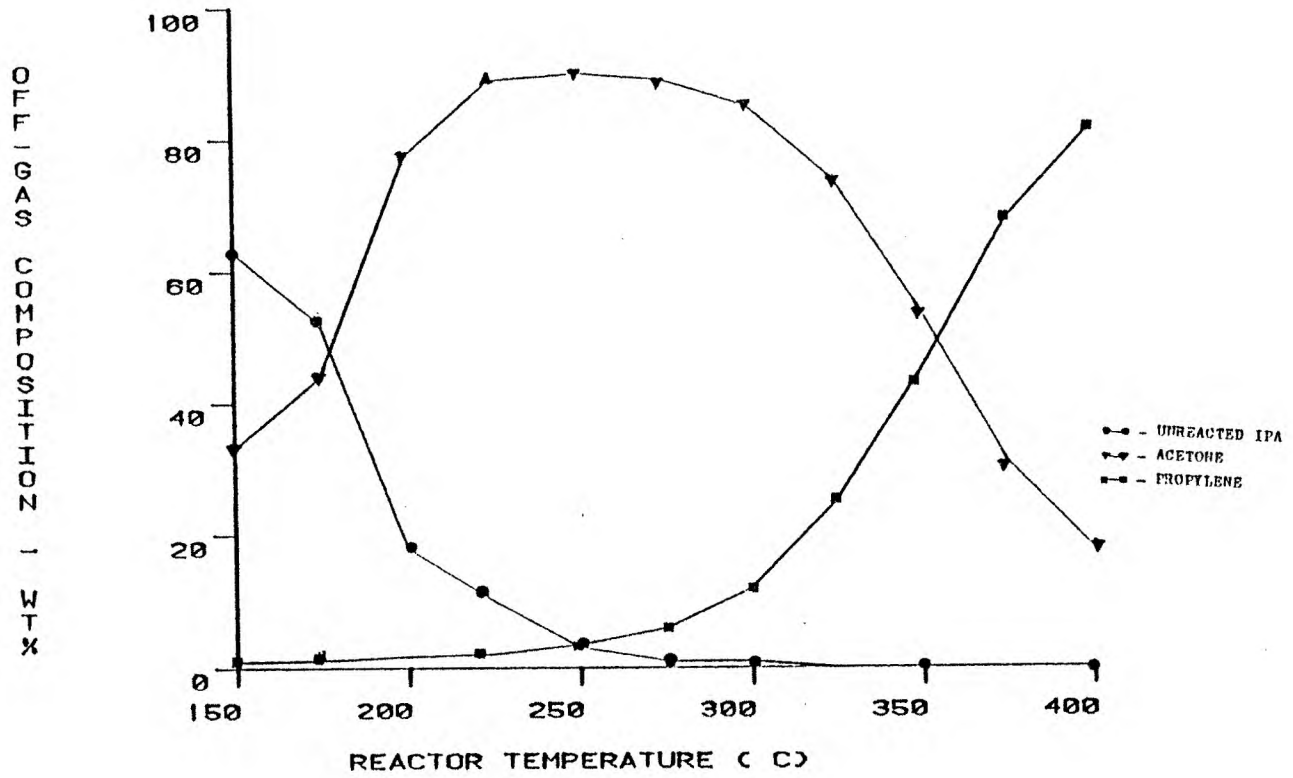

SEMI LOG PLOT FRACTION IPA REMAINING VS RESIDENCE TIME

A semi-log plot of $(1 - X_a)$ vs τ was made in order to check the assumed validity of first order reaction kinetics for the plug flow model. The linearity of figure 9 indicates that the assumption of first order was indeed valid over the experimental test conditions. It should be mentioned, however, that at high residence times, the curve flexes upward at each isotherm, and this may signal a change in the reaction control mechanism. Unfortunately, inadequate flow control and measurement at those low flow rates disallowed further study of this deep laminar region. These plug flow rates are shown in table 2 and figure 9.

Figure 9 also shows the affect of the amount of catalyst on the reaction rate. Runs made using one and two grams charge demonstrated equal conversions for identical residence times. This finding suggests the reaction conversion to be essentially chemical reactant rate controlling and not dependent upon amount of catalyst.

Figure 9. SEMILOG PLOT OF FRACTION IPA REMAINING
VS
RESIDENCE TIME

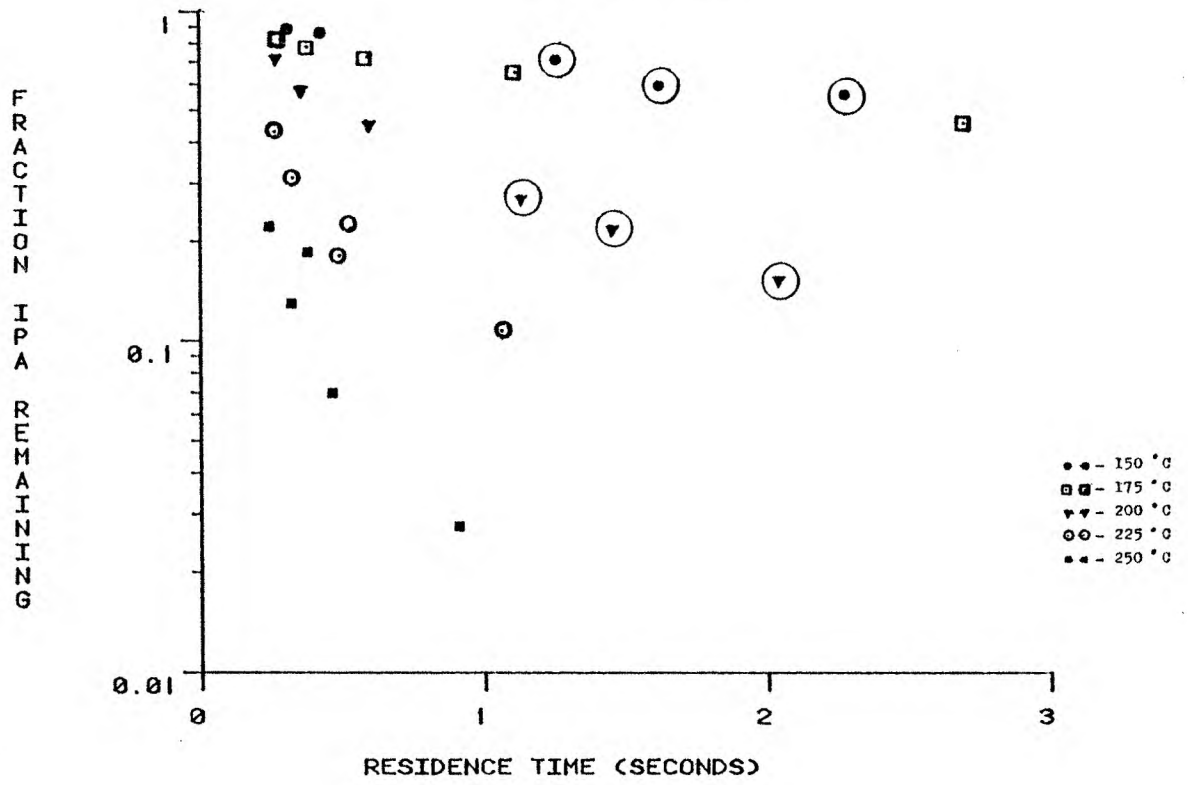

NOTE: Encircled symbol indicates two gram catalyst charge.

TABLE 2

Tabulation of Specific Rate Constants

(Dispersion and Plug Flow Models)

Pt.No.	Temp (°K)	Temp (°K)$^{-1}$ x(10^{-3})	Rate Constant (sec^{-1}) Dispersion Model	Rate Constant (sec^{-1}) Plug Flow Model	% Difference
42	423	2.364	0.102	0.102	0.0
41	423	2.364	0.174	0.174	0.0
5	423	2.364	0.218	0.217	0.5
4	423	2.364	0.277	0.274	1.1
3	423	2.364	0.215	0.212	1.4
	Average		0.197	0.196	0.6
	Standard Deviation		±0.058	±0.057	
36	448	2.232	0.406	0.405	0.2
35	448	2.232	0.475	0.455	0.4
34	448	2.232	0.417	0.413	1.0
33	448	2.232	0.320	0.314	1.9
32	448	2.232	0.284	0.261	8.1
	Average		0.377	0.370	2.3
	Standard Deviation		±0.064	±0.071	
31	473	2.114	0.901	0.895	0.7
30	473	2.114	1.282	1.263	1.5
29	473	2.114	1.215	1.180	2.9
10	473	2.114	1.097	1.071	2.4
9	473	2.114	1.030	0.995	3.4
8	473	2.114	0.928	0.877	5.5
	Average		1.076	1.047	2.7
	Standard Deviation		±0.139	±0.141	
26	498	2.008	2.967	2.899	2.3
25	498	2.008	3.446	3.328	3.4
24	498	2.008	2.879	2.719	5.6
23	498	2.008	2.320	2.028	12.6
44	498	2.008	3.550	3.336	6.0
	Average		3.032	2.862	6.0
	Standard Deviation		±0.441	±0.481	
21	523	1.912	6.050	5.790	4.3
20	523	1.912	6.408	6.013	6.2
19	523	1.912	6.018	5.460	9.3
18	523	1.912	4.650	3.814	18.0
45	523	1.912	4.480	4.246	5.2
	Average		5.521	5.065	9.6
	Standard Deviation		±0.794	±0.874	

DETERMINATION OF THE ARRHENIUS PARAMETERS

The reaction rate constants were computed by both the dispersion and plug flow models. Table 2 shows the specific reaction rate constant, k, calculated by both models and the standard deviation and percent difference between methods. There does not appear to be a significant difference in values of the specific rate constant despite the low Reynolds number used and the resulting higher dispersion number. Nonetheless, upon closer inspection, a deviant trend emerges as indicated by greater percent differences with increasing temperature. This occurrence suggests perhaps a significant departure from ideal plug flow characteristics at higher temperatures.

The observed activation energy and pre-exponential factor were determined using the average k-values obtained by both models. A semi-log plot of k versus 1/T was made and is shown in figure 10. The observed activation energy was obtained from the slope of the curve (using linear regression) and was found to be 15.36 kcal/gm-mole. Similarly, the pre-exponential factor was calculated from the y-intercept and its value was determined to be 1.453×10^{7} sec^{-1}. The graph shows that the values of specific rate constant, k, are essentially equal from both the plug flow and dispersion models.

Figure 10. DETERMINATION OF THE ARRHENIUS PARAMETERS

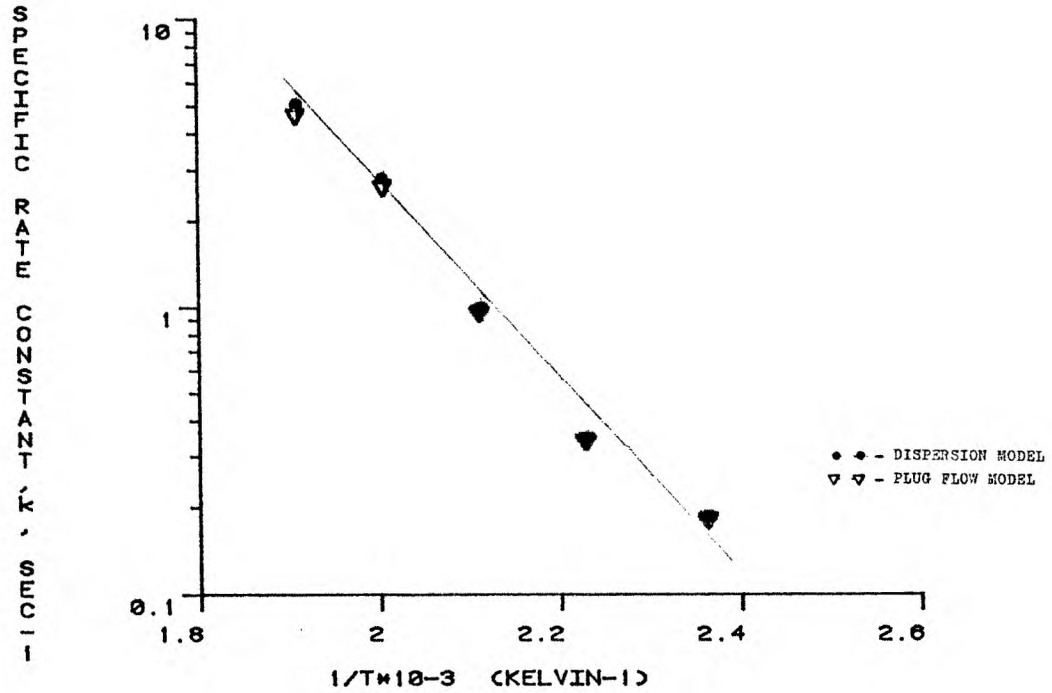

CHAPTER VI

CONCLUSIONS

On the basis of the experimental findings presented in the preceding chapters, the following conclusions are made:

1) The decomposition reaction of IPA over 0.5% platinum on charcoal exhibited first order reaction kinetics by both the plug flow and dispersion models.
2) The reaction rate was found to be directly proportional to the amount of catalyst used.
3) The catalytic decomposition of IPA to acetone occurred predominantly at low temperatures (below 350^{o}C) and short residence times. However, at temperatures above 350^{o}C and long contact times, formation favoring propylene was observed.
4) Catalyst decay was observed to occur at both high (above 400^{o}C) and low (below 150^{o}C) temperature levels. Sintering was suspected as the cause of high temperature irreversible deactivation, whereas fouling was felt to be responsible for low temperature reversible decay. At intermediate temperature conditions (150-400^{o}C), little to no deactivation was observed.
5) The activation energy (obtained using rate constants from the dispersion model) was found to equal 15.36 kcal/gm-mole. Similarly, the pre-exponential factor was determined to be 1.453×10^{7} sec^{-1} (based on bed void volume).

6) The activation energy (obtained using rate constants from the plug flow model) was found to equal 15.11 kcal/gm-mole. Similarly, the pre-exponential factor was determined to be 9.63×10^{6} sec^{-1} (based on bed void volume).

7) There is no statistically significant difference between data obtained using the dispersion model or the plug flow model for the dispersion number equal to or less than about 0.07.

CHAPTER VII

RECOMMENDATIONS

On the basis of the experimental findings discussed in preceding chapters, the following recommendations are made for further study.

1) Investigate sintering as possibly the main cause of high temperature deactivation--perform chemisorption surface studies on fresh and spent catalyst.
2) Study the dependence of reaction selectivity on residence time at various reactor temperatures.
3) Demonstrate the catalyst's impact on facilitating the decomposition reaction by conducting runs at various operating conditions without catalyst.
4) Assess the effect of diffusion upon reaction conversion by making runs employing various particle sizes.

APPENDICES

APPENDIX A

EXPERIMENTAL PROCEDURE

Operating Instructions

I. Preliminary Start-Up Procedure

1. Warm-up Hewlett-Packard Gas Chromatograph (to be done on the afternoon before the day of the run).

   a. Purge Gas Chromatograph by opening Cylinder "B" valve till pressure gauge reads 60 psig.

   b. Adjust the helium carrier gas flow to approximately 25 cc/min using knobs "A" and "B" on panel of Gas Chromatograph. Check flows with bubble buret.

   c. After 15 minutes of purge, set the

      Injection Port Temperature . . . 250°C
      Auxiliary Temperature . . . . . 250°C
      Detector Temperature . . . . . 250°C

   d. Open the Oven Temperature Programmer panel and set "DET 2"

      Time 1 . . . . . 0°C
      Temperature 1 . . . . . 85°C
      Rate, cc/min 0
      Time 2 . . . . . ∞
      Temperature 2 . . . . . 0°C

   e. Press line switch to "ON" (light on) and all three demand lights on control panel will flash on. Turn Oven Mode to Operate (oven demand light goes on).

   f. Push "SET NEW TEMP 1" button.

   g. Thermal equilibrium reached when all four demand lights flicker.

h. Set the Attenuation to infinity.

i. Set the Polarity on "B."

j. Set the Offset on "none."

k. Set the Sensitivity knob in Position 1.

l. Using the Meter Selector read and periodically monitor

- Oven Temperature
- Detector Temperature
- Injection Port Temperature
- Auxiliary Temperature
- TC Current (Detector Power Sensitivity)

m. Recheck carrier gas flow rate and readjust to 25 cc/min if necessary.

--Gas Chromatograph is now ready for overnight warm-up--

2. Reactor Warm-up/Catalyst Thermal Cleaning Procedure (same day).

a. Turn Cylinder "A" valve open till pressure gauge reads 50 psig. Close both valves on top of spargers.

b. Turn the six-way valve to the right (Flow to Reactor).

c. Adjust flow rate on Rotameter ER till stainless steel (s.s.) bob holds steady at 35.

d. Switch Temperature recorder "ON." Set Chart Recorder to "LOW" speed.

e. Turn on the variac and set at 33 (temperature will equilibrate at about 260^{o}C).

f. Track reactor temperature rise on Chart Recorder. When temperature ascent appears steady, turn off Recorder.

--Reactor warm-up procedure is now complete--

--Leave on overnight to permit thermal cleaning of catalyst--

II. Run Start-Up Procedure (next morning)

1. Equipment Operating Stability Check and Final Purge.

a. Turn on the Temperature Recorder. (Note reactor temperature.)

b. Check Gas Chromatograph flow rates. Adjust carrier gas flow control knobs "A" and "B" to ACCURATELY deliver 25 cc/min to each column. Check flows with bubble buret.

c. Reset the flow rate on Rotameter ER to 65 (ss bob).

d. Turn the Variac setting to 40 (temperature 280-300°C). Leave at 40 for about 90 minutes (Final purge).

e. Turn the Gas Chromatograph Sensitivity knob to 5.

f. Switch Variac power to "OFF." Allow the Reactor to cool down to run target temperature. When this temperature is reached, switch Variac "ON" and adjust to one of the five steady-state temperature settings below.

Target Temperature	Variac Steady-State Temperature Setting
150	23
175	26
200	28
225	31
250	33

Hold the reactor temperature constant. Correct for temperature drifting as necessary. (Thermal equilibrium reached in about one hour.)

g. Turn Rotameter ER OFF. (Final purge now complete.)

III. Runs

1. To Make a Run

a. Fully open valves on the top of both Spargers.

b. Set flow rate on Rotameter ES at 150 (s.s. bob, leave it on for 15 minutes).

c. Reset Rotameter ES to highest targetted flow rate. Accurately measure the flow rate using the bubble buret.

d. Every 15-20 minutes sample the reactor product stream and analyze it using the Gas Chromatograph. Compute and compare the compositions of the key components--namely, IPA, acetone, and propylene over time. When the compositions remain essentially unchanged, equilibrium is reached. (Equilibrium normally takes 90 minutes from step c.)

e. Take two equilibrium reactor product analysis samples according to the "Reactor Product Stream Analysis" method forthcoming (2.).

f. Take two reactor feed samples by the "Reactor Feed Analysis" method outlined in 3.

2. Reactor Product Stream Analysis

a. Turn the Loop Knob on top of the Gas Chromatograph to Opposite Position. Simultaneously, press the Integrator Buttons:

1. Start Analysis
2. Integrate
3. Print Time
4. Print Area

The components at 25 cc/min and the Gas Chromatograph Conditions Set will be:

Time, Sec	Component
75-85	Acetone
120-130	Isopropyl Alcohol

b. Push "Stop Analysis" when all components have been eluted (about 5 minutes). Repeat procedure for second sample.

3. Reactor Feed Analysis

a. Turn the Reactor six-way valve to the left for the feed analysis. Wait five minutes for a complete purge.

b. Turn the Loop Knob to opposite position and push the integrator buttons

1. Start Analysis

2. Integrate
3. Print Time
4. Print Area

c. After all components have been eluted from the Gas Chromatograph, repeat again for second sample.

d. Turn Reactor six-way valve to right. Lower Rotameter ES Setting to deliver next targetted flow rate. Continue next run by going back to step 1d.

4. Calibration of Gas Chromatograph (to be done at end of day)

a. Inject 1 ul of Isopropyl Alcohol (liquid) into Sampling Port "B." (Use Hamilton Syringe model #1701.) Simultaneously, press the Integrator Buttons

1. Start Analysis
2. Integrate
3. Print Time
4. Print Area

b. Repeat the procedure four additional times in order to obtain an average of five Integrator Readings. (The use of this Average Reading is shown in Appendix C.)

IV. Shutdown Procedure

1. Turn Off the Instruments First

a. Turn off the Integrator

b. Turn off the Gas Chromatograph Recorder. Set the chart speed to "OFF."

c. Set the Detector Power sensitivity to "OFF."

d. Set the Attenuation to ∞.

e. Set the Detector Temperature to "OFF."

f. Set the Auxiliary Temperature to "OFF."

g. Set the Injection Port Temperature to "OFF."

h. Set the Oven Mode to "OFF." (All demand lights should now be off.)

i. Set the line switch to "OFF."

2. Reactor

a. Turn the reactor Variac to "Zero" and turn off the power.

3. Gas Flow

a. Turn off the gas flow to the Spargers by setting Rotameter ES to "Zero."

b. Close the valves at the top of the Spargers.

c. Turn on the flow rate to flowmeter ER and set at 65 (s.s. bob).

d. Allow helium to flow through the system for 45 minutes.

e. Shut off the flowmeter ER.

4. Temperature Recorder

a. Shut off the Temperature Recorder.

5. Shut Off Cylinder "A"

6. Shut Cylinder "B" Off the Next Morning

--The run is now complete--

--Next run can be conducted at a new targeted temperature--

(I.E. 250, 225, 200, 175, or 150°C)

APPENDIX B

DATA BASE DEVELOPMENT

(Typical Data Sheet & Sample Calculations)

Data Point No. 31

I. Data Sheet

A. Analytical Equipment Check: (after overnight warm-up)

1. Gas chromatograph:

a) column temperature . . . . . 85°C
b) carrier flowrate . . . . . 25 cc/min
c) carrier feed pressure . . . . . 60 psig
d) detector temperature . . . . . 250°C
e) injection port temperature . . . 250°C
f) auxiliary temperature . . . . . 250°C
g) sensitivity . . . . . 164mA(setting 5)
h) attenuation x8

2. Integrator:

a) operating mode . . . . . automatic
b) sensitivity . . . . . 3(1-low, 4-high)

B. Experimental Conditions: (at steady state)

1. Reactor conditions:

a) temperature . . . . . 200°C
b) pressure . . . . . 1 psig
c) volumetric flowrate . . . . . 187 cc/min (@ rm temp)

2. Catalyst bed properties:

a) amount of catalyst . . . . . 1.00 gram
b) bed length . . . . . 3.215 cm
c) void fraction 0.529

3. Ambient condition:

a) room temperature . . . . . 25°C

4. Control settings:

a) rotameter setting . . . . . 150 (s.s. bob)

b) gas pressure (to rotameter) . . 50 psig

c) variac setting (for reactor) . . 29 volts

C. Steady State Assessment

To trace the pathway to stable operation, reactor off-gases were periodically sampled and sent to the chromatograph for analysis. Values of weight percent acetone were then computed and listed in tabular form against sampling time. When three consecutive values (of weight percent acetone) remained essentially unchanged---the condition of steady state was reached, and the data point was then obtained.

Approach to Steady State

Time (sec)	Wt % Acetone
0	19.98
1206	20.47
2133	20.17
2919	19.69
3505	19.97

Establishing stable operation

D. Final Steady State Values (data pt. #31)

Unreacted isopropyl alcohol (IPA) in reactor off-gas (average of both sampling loops) 28225*

IPA in feed gas 35935*

Percentage of feed converted:

$$X_a = (1 - 28225/35935) \times 100 = 21.45\%$$

*Note: This number represents the integrator reading.

APPENDIX C

SAMPLE CALCULATIONS

(DATA PT #31)

A. Estimate Reynold's (N_{re}) and Schmidt (N_{sc}) Numbers

1. Find feed gas density

   a) Compute average of integrator readings (I.R.'s) of IPA in feed gas for both sampling loops.**

	I.R.'s
Loop 1:	37110
Loop 2:	34760
Average	35935

**Note: For reason of precision--though both sampling loops were rated to contain a 1/2 cc sample, I.R.'s consistently indicated a 5% difference in volume.

   b) Obtain comparative standard I.R. by injecting 1 ul of IPA into chromatograph:

Injection #	I.R.'s
(1)	754200
(2)	708400
(3)	738200
(4)	729800
(5)	749000
Average	735920

   c) Proportion both standard and feed I.R.'s to determine the amount of IPA contained in the feed sampling loop:

$$\frac{\text{Avg I.R. of feed loop}}{\text{Avg I.R. of 1 ul injection}} = \frac{35935}{735920} = \frac{X}{1 \text{ ul}}$$

$\therefore$ Amount IPA contained in loop = X = 0.0488 ul $\equiv 0.0488 \times 10^{-3}$ cc

gm-moles of IPA =

$$= (0.0488 \times 10^{-3}\text{cc})(0.786\ \text{gm/cc})(1\ \text{gm-mole}/60.1\ \text{gm})$$

$$= 6.386 \times 10^{-7}\ \text{gm-moles}$$

$$\text{volume of IPA in loop} = \frac{nRT}{P} =$$

$$(6.386 \times 10^{-7}\ \text{gm-moles})\left(82.06\ \frac{\text{atm-cc}}{\text{gm-mole-}^\circ\text{K}}\right)$$

$$\frac{x(250 + 273)^\circ\text{K}}{1\ \text{atm}}$$

$$= 0.0274\ \text{cc}$$

d) Find amount of helium in sampling loop:

volume of He = loop volume - volume of IPA

V_{He} = 0.5 cc - 0.0274 cc = 0.4726 cc of He

gm-moles of He =

$$\frac{PV}{RT} = \frac{(1\ \text{atm})(0.4726\ \text{cc})}{\left(82.06\ \frac{\text{atm-cc}}{\text{gm-mole-}^\circ\text{K}}\right)(250 + 273)^\circ\text{K}}$$

$$= 1.10 \times 10^{-5}\ \text{gm-moles}$$

e) Calculate feed gas density (ρ)

(density (250°C) = mass sum of constituents divided by loop volume)

$$= \frac{(1.1 \times 10^{-5}\text{gm-moles})(4\ \text{gms/gm-mole}) +}{(0.5\ \text{cc})}$$

$$\frac{(6.386 \times 10^{-7}\text{gm-mole})(60.1\ \text{gms/gm-mole})}{(0.5\ \text{cc})}$$

$$= 1.649 \times 10^{-4}\ \text{gm/cc}$$

f) Adjust density to reactor temperature (200°C):

$$\text{density (200°C)} = \text{density (250°C)} \frac{\text{loop temperature °K)}}{\text{(reactor temperature °K)}}$$

$$= 1.649 \times 10^{-4} \text{gm/cc} \ \frac{(250 + 273)}{(200 + 273)}$$

$$= 1.823 \times 10^{-4} \text{gm/cc}$$

2. Find viscosity (u):

viscosity = 0.026 cP for pure helium at 200°C (Perry's Hdbk)

(converting to consistent units)

$$0.026 \text{ cP} \times 1.0 \times 10^{-2} \text{gm/(cm-sec)-cP}$$

$$= 0.00026 \text{ gm/cm-sec}$$

3. Average particle diameter (d_p):

$$d_p = 0.313 \text{ cm (as per Appendix E)}$$

4. Superficial velocity (v_s):

(Volumetric flowrate (v) adjustment to 200°C)

$$\text{(200°C)} = 187 \text{ cc/min} \ \frac{(200 + 273)}{(25 + 273)}$$

$$= 296.8 \text{ cc/min}$$

$$v_s = \frac{\text{volumetric flowrate}}{\text{reactor inside cross-sectional area}}$$

$$= \frac{296.8 \text{ cc/min}}{\pi \ \frac{(1 \text{ cm})^2}{4} \ (60 \text{ sec/min})} = 6.30 \text{ cm/sec}$$

5. Diffusivity ($\mathcal{D}_{ah}$) of IPA in He:

$\mathcal{D}_{ah}$ (150°C) = 0.677 cm^2/sec (Reid, Prausnitz, and Sherwood)

(adjusting to reactor temperature (200°C))

$$\mathcal{D}_{ah}\ (200°C) = \mathcal{D}_{ah}\ (150°C)(\text{reactor temp}/(150+273))^{3/2}$$

$$= 0.677\ cm^2/sec\ \frac{(200+273)^{3/2}}{(150+273)}$$

$$= 0.80\ cm^2/sec$$

6. Estimation of N_{re}:

$$N_{re} = \frac{d_p \times v_s \times \rho}{u}$$

$$= \frac{(0.313\ cm)(6.30\ cm/sec)(1.823 \times 10^{-4} gm/cc)}{(0.00026\ gm/cm\text{-}sec)}$$

$$= 1.383$$

7. Estimation of N_{sc}:

$$N_{sc} = u/\rho\ \mathcal{D}_{ah}$$

$$= \frac{(0.00026\ gm/cm\text{-}sec)}{(1.823 \times 10^{-4} gm/cc)(0.80\ cm^2/sec)}$$

$$= 1.783$$

B. Determine Rate Constant (k) via Dispersion Model

1. Compute axial peclet number (N_{pe_a}):

Using equation 5-36 in Wen and Fan, for gases flowing through packed beds:

$$\frac{1}{N_{pe_a}} = \frac{\varepsilon\gamma}{N_{sc} \cdot N_{re}} + \frac{0.5}{(1 + \varepsilon(\beta)(N_{re} \cdot N_{sc})^{-1}}$$

for $0.008 < N_{re} < 400$ and $0.28 < N_{sc} < 2.2$

where: ε = bed void fraction = 0.529

$\gamma = 0.75$

$\beta = 9.5$

$$\frac{1}{N_{pe_a}} = \frac{0.529(0.75)}{(1.783)(1.383)} + \frac{0.5}{(1 + 0.529(9.5))(1.383 \times 1.783)^{-1}}$$

$$= 0.3256$$

or

$$N_{pe_a} = 3.07$$

2. Calculate axial dispersion group:

a) Find axial dispersion coefficient (D_z):

$$N_{pe_a} = \frac{\text{(superficial velocity)(particle diameter)}}{\text{(dispersion coefficient)}}$$

$$= v_s \cdot d_p / D_z$$

$$D_z = v_s \cdot d_p / N_{pe_a}$$

$$= \frac{(6.30 \text{ cm/sec})(0.313 \text{ cm})}{(3.07)}$$

$$= 0.642 \text{ cm}^2/\text{sec}$$

b) Calculate reciprocal axial dispersion group $(\frac{v_s L}{D_z})$

reciprocal axial dispersion group =

$$\frac{\text{(superficial velocity)(bed length)}}{\text{(dispersion coefficient)}}$$

$$= \frac{(6.3 \text{ cm/sec})(3.215 \text{ cm})}{(0.642 \text{ cm}^2/\text{sec})}$$

$$= 31.55$$

3. Calculate residence time (τ):

$$\tau = \frac{\text{(bed void volume)}}{\text{(volumetric flowrate)}} = \frac{\pi(1 \text{ cm})^2(3.215 \text{ cm})(0.529)}{(4)\ \frac{(296.8 \text{ cc/min})}{(60 \text{ sec/min})}}$$

$$= 0.27 \text{ sec}$$

4. Solve for "a":

solved via TI-58 calculator program (see Appendix G)

$$a = 1.01531$$

5. Solving for k via dispersion model***

$$k = \frac{a^2 - 1}{4(\tau)(\frac{D_z}{v_s L})} = \frac{(1.01531)^2 - 1}{4(0.27\ \text{sec})(1/31.55)}$$

$$= 0.901\ \text{sec}^{-1}$$

***Note: k is based on void fraction

C. Determine Rate Constant (k) via Plug Flow Model

$$\frac{\text{void volume}\ \varepsilon(Vb)}{\text{molar feed rate}} = \int_{X_{a_i}}^{X_{af}} \frac{dX_a}{(-r_a)} = \int_{X_{a_i}}^{X_{af}} \frac{dX_a}{k\ C_{ai}(1 - X_a)}$$

$$\frac{\varepsilon V_b}{v_i C_{ai}} = \int_{X_{a_i}}^{X_{af}} \frac{dX_a}{k\ C_{ai}(1 - X_a)} = -\frac{\ln(1 - X_a)}{k}\Bigg|_{X_i = 0}^{X_f = .2145}$$

or

$$k = -\frac{\ln(1 - .2145)}{0.27\ \text{sec}} = 0.895\ \text{sec}^{-1}$$

% difference from dispersion model estimate:

$$\frac{(0.901 - 0.895)}{0.901} \times 100 = 0.67\%$$

APPENDIX D

ESTIMATION OF BED LENGTH

Bed length was estimated via average bulk bed density (ρ_b). For reason of accuracy, ρ_b's were determined for both packed and unpacked beds. These values were then averaged to obtain an average ρ_b.

All catalyst bed measurements were made using a Pyrex glass graduated cylinder (No. 3022, 1-10 cc; i.d. of graduated cylinder $\cong$ i.d. of reactor).

Test	Weight (in grams) of 10 cc of Catalyst	
	Packed Bed	Unpacked Bed
1st	4.28	3.72
2nd	4.17	3.81
3rd	4.12	3.64
Average	4.19	3.72
Overall Average	3.96	

$$\text{Average Bulk density} = \frac{3.96 \text{ gms}}{10 \text{ cc}} = 0.396 \text{ gms/cc}$$

$$\text{Bed Length} = \frac{(\text{bulk density})^{-1}(\text{catalyst charge weight})}{(\text{reactor inside cross-sectional area})}$$

$$= \frac{(1/0.396 \text{ gms/cc})(1 \text{ gm})}{\frac{\pi}{4}(1 \text{ cm})^2} = 3.215 \text{ cm}$$

APPENDIX E

ESTIMATION OF AVERAGE PARTICLE DIAMETER

Sieve Tray Analysis

Col 1 Tray Size	Col 2 Screen Opening	Col 3 Weight (grams)	Col 4 Weight Fraction	Col 2 x Col 4 Average Particle Diameter (inches)
#5	0.157	2.44	0.240	0.0376
#6	0.132	2.32	0.229	0.0300
#7	0.111	3.71	0.367	0.0406
#8	0.0937	1.25	0.124	0.0115
Pan	0.09	0.41	0.040	0.0036
		Σ = 10.13	Σ = 1.00	Σ = 0.1233

$\therefore$ Average Particle Diameter $\cong$ 0.313 cm

APPENDIX F

ESTIMATION OF BED VOID FRACTION

The procedure used to determine the bed void fraction is as follows:

1) Fill graduate (No. 3022) with catalyst to 10 cc mark.
2) Remove and weigh catalyst.
3) Soak catalyst in water till effervescence subsides (i.e., point of saturation).
4) Remove catalyst from water and gently tap dry surface with paper towel to sponge-off excess moisture.
5) Reweigh catalyst.
6) Add catalyst back to graduate.
7) Add water slowly to graduate/catalyst bed to displace air entrapped in voids.
8) Stop water addition when 10 cc mark is reached.

Finally, the volume of water added divided by the total bed volume, equals the void fraction. This value was found to be 0.529.

APPENDIX G

TEXAS INSTRUMENTS PROGRAMMABLE CALCULATION RECORD FOR COMPUTATIONS OF THE CONSTANT "a" IN EQUATION 6 IN THE DISPERSION MODEL FOR FIRST ORDER REACTION

A fast convergence scheme (linear interpolation) to solve for "a" in equation 6.

User Instructions

Step	Procedure	Enter	Press	Display
1	Clear All Memory Registers		2nd CMs	00
2	Store Conversion (e.g. .2145)	.2145	Sto 02	.2145
3	Store Reciprocal Dispersion No. (e.g. 31.55)	31.55	Sto 01	31.55
4	Store Tolerance (recommend .00001)	.00001	Sto 17	.00001
5	Store initial guess for "a" (recommend 1.1)	1.1	Sto 00	1.1
6	Set x ⇄ t (T-register) at 1	1	x ⇄ t	
7	Reset Program		RST	
8	Start Program (in about 3 min calculation ended)		R/S	.0000055919
9	Recall "a"		Rcl 00	1.01530299

Data Registers

x ⇄ t: 1

0	"a"
1	Reciprocal Dispersion No. $v_s L/D_z$
2	Conversion (fraction)
17	tolerance (.00001)

Solving for "a" via Linear Interpolation

Location	Code	Key
00	04	4
01	65	X
02	43	Rcl
03	00	00
04	65	X
05	53	(
06	93	•
07	05	5
08	65	X
09	43	Rcl
10	01	01
11	54	)
12	22	Inv
13	23	Lnx
14	95	=
15	42	Sto
16	10	10
17	53	(
18	01	1
19	85	+
20	43	Rcl
21	00	00
22	54	)
23	33	X^2
24	65	X
25	53	(
26	43	Rcl
27	00	00
28	65	X
29	93	•
30	05	5
31	65	X
32	43	Rcl

Location	Code	Key
33	01	01
34	54	)
35	22	Inv
36	23	Lnx
37	75	-
38	53	(
39	01	1
40	75	-
41	43	Rcl
42	00	00
43	54	)
44	33	x^2
45	65	X
46	53	(
47	53	(
48	43	Rcl
49	00	00
50	65	X
51	93	.
52	05	5
53	65	X
54	43	Rcl
55	01	01
56	54	)
57	94	±
58	22	Inv
59	23	Lnx
60	54	)
61	95	=
62	42	Sto
63	11	11
64	43	Rcl
65	10	10
66	55	÷

Location	Code	Key
67	43	Rcl
68	11	11
69	75	-
70	53	(
71	01	1
72	75	-
73	43	Rcl
74	02	02
75	54	)
76	95	=
77	42	Sto
78	12	12
79	43	Rcl
80	09	09
81	67	x=t
82	01	1
83	11	11
84	43	Rcl
85	12	12
86	95	=
97	42	Sto
88	13	13
89	43	Rcl
90	00	00
91	95	=
92	42	Sto
93	06	06
94	43	Rcl
95	00	00
96	65	X
97	01	1
98	93	.
99	00	0
100	05	5
101	95	=

Location	Code	Key
102	42	Sto
103	00	00
104	01	1
105	95	=
106	42	Sto
107	09	09
108	61	GTO
109	00	00
110	00	00
111	53	(
112	43	Rcl
113	13	13
114	75	-
115	43	Rcl
116	12	12
117	54	)
118	55	÷
119	53	(
120	43	Rcl
121	06	06
122	75	-
123	43	Rcl
124	00	00
125	54	)
126	95	=
127	42	Sto
128	14	14
129	43	Rcl
130	13	13
131	75	-
132	43	Rcl
133	14	14
134	65	X
135	43	Rcl
136	06	06

Location	Code	Key
137	95	=
138	42	Sto
139	15	15
140	53	(
141	43	Rcl
142	15	15
143	55	÷
144	43	Rcl
145	14	14
146	54	)
147	94	±
148	95	=
149	42	Sto
150	00	00
151	43	Rcl
152	17	17
153	32	x ⇄ t
154	53	(
155	43	Rcl
156	00	00
157	75	-
158	43	Rcl
159	06	06
160	54	)
161	50	|x|
162	22	Inv
163	77	x ≥ t
164	01	1
165	90	90
166	42	Sto
167	09	09
168	01	1
169	32	x ⇄ t
170	61	GTO
171	00	00
190	91	R/S

APPENDIX H

TABLE 3

Tabulation of Data

Point No.	Volumetric Throughput (cc/sec)	Superficial Velocity (cm/sec)	Residence Time (sec)	N_{RE}	N_{SC}	N_{Pea}	Dispersion Coefficient (cm^2/sec)	Dispersion Group	Reactor Temp (^oC)	X Conversion (%)
42	4.32	5.50	0.309	1.40	1.82	3.09	0.558	0.0315	150	3.1
41	3.11	3.96	0.430	1.04	1.75	2.86	0.434	0.0341	---	7.2
5**	2.11	2.68	1.267	0.75	1.66	2.39	0.352	0.0204	---	24.0
4**	1.64	2.09	1.629	0.59	1.63	2.04	0.321	0.0239	---	36.0
3**	1.17	1.49	2.281	0.43	1.60	1.57	0.297	0.0396	---	38.3
36	4.67	5.95	0.286	1.46	1.73	3.08	0.604	0.0315	175	10.9
35	3.50	4.45	0.382	1.10	1.71	2.88	0.483	0.0338	---	15.9
34	2.25	2.86	0.595	0.71	1.67	2.36	0.380	0.0413	---	21.8
33	1.20	1.53	1.115	0.39	1.68	1.49	0.320	0.0652	---	29.5
32	0.49	0.64	2.700	0.16	1.67	0.67	0.298	0.1458	---	50.6
31	4.95	6.30	0.270	1.38	1.78	3.07	0.642	0.0316	200	21.5
30	3.60	4.58	0.371	1.03	1.75	2.83	0.505	0.0344	---	37.4
29	2.22	2.83	0.601	0.65	1.70	2.23	0.397	0.0437	---	50.8
10**	2.36	3.00	1.134	0.68	1.72	2.31	0.406	0.0211	---	70.3
9**	1.83	2.33	1.457	0.53	1.71	1.95	0.373	0.0249	---	76.5
8**	1.31	1.67	2.040	0.38	1.70	1.50	0.347	0.0324	---	83.3
26	5.06	6.44	0.264	1.26	1.85	3.04	0.662	0.0319	225	53.5
25	4.08	5.20	0.327	1.03	1.83	2.88	0.564	0.0338	---	66.4
24	2.52	3.20	0.531	0.65	1.79	2.29	0.437	0.0426	---	76.4
23	1.26	1.60	1.062	0.33	1.77	1.36	0.369	0.0719	---	88.4
44	2.72	3.46	0.490	0.60	2.08	2.40	0.451	0.0405	---	80.5
21	5.45	6.94	0.245	1.27	1.84	3.04	0.714	0.0319	250	75.8
20	4.08	5.20	0.327	0.96	1.82	2.81	0.579	0.0346	---	86.0
19	2.83	3.60	0.472	0.68	1.79	2.35	0.479	0.0414	---	92.4
18	1.46	1.86	0.916	0.35	1.77	1.45	0.402	0.0671	---	97.0
45	3.53	4.50	0.378	0.76	1.99	2.65	0.532	0.0368	---	79.9

NOTE: Double asterisk (**) denotes two (2) grams of catalyst was charged to the reactor. Otherwise, one (1) gram charge is understood.

TABLE 4

Data for Figure 4

Reaction Selectivity as Impacted By Catalyst Decay
Reactor OFF-GAS Composition (WT%) vs Reactor Temperature (^{o}C)

Temp	Unreacted IPA		Acetone		Propylene	
	Fresh	Spent	Fresh	Spent	Fresh	Spent
150	63	82	33	17	1	1
175	52	73	44	26	1.2	1.2
200	18	45	77.5	53	1.7	1.7
225	10	22	89	76	2.1	2.1
250	3	8.5	90	89	3.5	2.5
275	1	3.5	89	93	6.0	4.0
300	1	2	85	91	12.0	6.0
325	0	1	74	88	25.0	12.0
350	0	0	54	80	45.0	19.0
375	0	0	31	70	68	29.0
400	0	0	18	60	82	40.0

TABLE 5

Data for Figure 5

Typical High Temperature (400°C) Deactivation Curve
Acetone in OFF-GAS (Wt %) vs Time (sec)

Time	Wt % Acetone
0	22
1000	36
2000	45
3000	50
4000	54
5000	56
6000	60
7000	63
8000	64
9000	66

TABLE 6

Data for Figure 8

Reaction Selectivity as a Function of Temperature

Temp (° C)	Unreacted IPA	Acetone	Propylene
150	63	33	1.0
175	52	44	1.2
200	18	77.5	1.7
225	10	89	2.1
250	3	90	3.5
275	1	89	6.0
300	1	85	12.0
325	0	74	25.0
350	0	54	45.0
375	0	31	68.0
400	0	18	82.0

TABLE 7

Data for Figure 9

Semilog Fraction IPA Remaining vs Residence Time (second)

Temp (°C)	Fraction Remaining	τ(sec)
150	.969	.309
	.928	.430
	*.76	1.267
	*.64	1.629
	*.617	2.281
175	.891	.286
	.841	.382
	.782	.595
	.705	1.115
	.494	2.700
200	.785	.270
	.626	.371
	.492	.601
	*.297	1.134
	*.235	1.457
	*.167	2.040
225	.465	.264
	.336	.327
	.236	.531
	.116	1.062
	.195	.490
250	.242	.245
	.140	.327
	.076	.472
	.030	.916
	.201	.378

*2 gram catalyst charge

TABLE 8

Data for Figure 10

Determination of the Arrhenius Parameters

ln k vs 1/T

	k (sec^{-1})	
$1/Tx10^{-3}(^{o}K^{-1})$	Dispersion	PFM
2.364	0.197	0.196
2.232	0.377	0.370
2.114	1.076	1.047
2.008	3.032	2.862
1.912	5.521	5.065

NOMENCLATURE

C	concentration, gm-moles/cm^3
d	diameter, cm
D_z	dispersion coefficient, cm^2/sec
$\mathcal{D}_{ah}$	diffusivity of IPA in He, cm^2/sec
F	molar flow rate, gm-moles/min or gm-moles/sec
k	specific reaction rate constant, sec^{-1}
ℓ	length, cm
L	reactor bed length, cm
n	reaction order
(-r)	rate of reaction
R	universal gas constant
T	temperature ^oK
u	viscosity, cP or gm/cm-sec
V	volume, cm^3
v	volumetric flowrate, cm^3/sec or cm^3/min
v_s	superficial velocity, cm/sec or cm/min
X	fractional conversion
Z	dimensionless bed length (ℓ/L)

Subscripts

a	refers to isopropyl alcohol
b	reactor bed
f	final or reactor exit condition
h	refers to helium
i	initial or reactor entrance condition
p	catalyst particle

Greek Symbols

ε bed void fraction

ρ density, gm/cm^3

τ residence time, sec (based on interstitial velocity)

Abbreviations

N_{re} Reynold's number

N_{sc} Schmidt number

N_{pe_a} axial Peclet number

IPA isopropyl alcohol

He helium

Selected Bibliography

1. Andersen, James B., A Chemical Reactor Laboratory for Undergraduate Instruction, Dept. of Chemical Engineering, Princeton University, Princeton, New Jersey, September 1968.

2. Carbery, James J., Chemical and Catalytic Reaction Engineering: McGraw-Hill, Inc., New York, 1976.

3. Froment, G.F. and Bischoff, K.B., Chemical Reactor Analysis and Design: John Wiley and Sons, New York, 1979.

4. Hatch, L.F., Isopropyl Alcohol: McGraw-Hill, New York, 1961.

5. Hughes, Thomas R., Advances in Analytical Chemistry I, Salt Lake City Conference, Snowbirt, Utah, Oct. 3-5, 1979.

6. Kokes, R.J., Tobin, H. and Emmett, P.H., J.A.C.S. 77, pp. 5860, 1955.

7. Levenspiel, Octave, Chemical Reaction Engineering: John Wiley & Sons, Inc., New York, 1972.

8. Perry, R.H. and Chilton, C.H., Chemical Engineers' Handbook, 1973.

9. Reid, R.C., Prausnitz, J.N., and Sherwood, T.K., The Properties of Gases and Liquids, 3rd Ed., pp. 558, McGraw-Hill Book Company, New York, 1977.

10. Smith, J.M., Chemical Engineering Kinetics: McGraw-Hill Book Co., New York, 1970.

11. Somorjai, G.A., "The Surface Structure of and Catalysis by Platinum Single Crystal Surfaces," Catalysis Reviews, Vol. 6, pp. 104, 1972.

12. Strau, David R. and Braun, Lee F., "Catalytic Reactor and Fouling Effects on Intraparticle Diffusion," J. of Catalysis, Vol. 32, pp. 37-49, 1974.

13. Wanke, S.E. and Flynn, P.C., "The Sintering of Supported Metal Catalysts," Cat. Reviews, Vol. 12, 1975.

14. Wen, C.Y. and Fan, L.T., "Models for Flow Systems and Chemical Reactors," Vol. 3, New York: Marcel Dekker, Inc., pp. 167-173, 1975.

15. Yashiva, Suzuki, and Hara, "Decomposition of 2-propanol over Alkali Cation Exchange Zeolites," J. of Catalysis, Vol. 33, pp. 486, June, 1974.